

Graphite and beta2-microglobulin

Maria Celeste Maschio

May 16, 2018

Experimental work of reference ([Mangione et al., 2013](#))

Focus is on D76N, the most amyloidogenic variant of b2m that is able to form readily amyloid fibrils in vitro under physiological extracellular conditions.

For this variant, the most common configuration of the His31-Pro32 bond is the non-native *trans*.

When interacting with a hydrophobic/hydrophilic interface, the protein is perturbed by several interactions: the most relevant is the hydrophobic force. One of the triggering factor is the exposition of hydrophobic domains.

The model to describe the hydrophobic interaction energy between two apolar surfaces is :

$$E_{hydro} = -2\gamma (a - a_0) \exp\left(-\frac{d}{D_{hydro}}\right)$$

and then the hydrophobic force acting on the molecule is calculated as:

$$F_{hydro} = -\left(\frac{dE_{hydro}}{dd}\right) = \frac{\left(-2\gamma(a-a_0) \exp\left(-\frac{d}{D_{hydro}}\right)\right)}{D_{hydro}}$$

considering the interfacial tension $\gamma = \frac{50mJ}{m^2}$, the exposed area $a_0 = 50 \text{ A}^2$, the hydrophobic decay length $D_{hydro} = 10 \text{ A}$, and $a(d) = \left(a_0 \left(1 - \exp\left(-\frac{d}{D_{hydro}}\right)\right)\right)^{-\frac{1}{2}}$ it is possible to find, for a distance between 1 and 10 A, that the energies vary $E_{hydro} = 14.7 - 0.7 \frac{kcal}{mol}$ and the forces between $F_{hydro} = 4.8 - 102 \text{ pN}$.

These intensities are strong enough to perturb the threedim structure of the b2m protein.

Contrarily to the wild type, D76N rapidly aggregates when agitated at 37.0°C, pH7.4 and in the presence of air/water interface (known to behave as a hydrophobic interface).

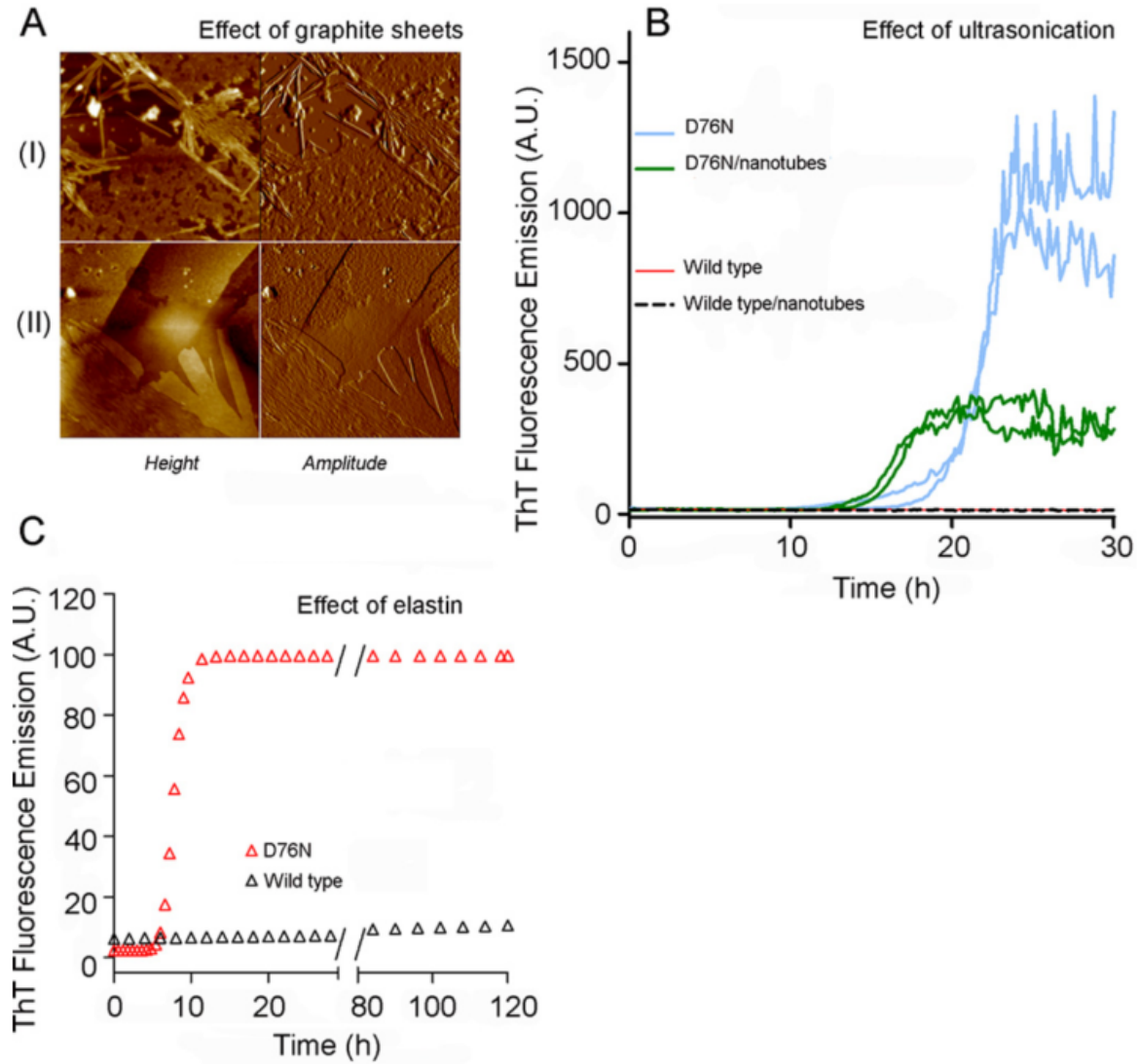


Figure 1: Fibrillogenesis of D76N and WT in presence of hydrophilic-hydrophobic interfaces. A, tapping mode AFM images of fibrils formed by D76N in the presence of graphite sheets under stirring conditions (I) or without agitation (II). B, time course of fibril formation by D76N under ultrasonication (light blue lines show replicate experiments) in contrast to the absence of fibrillogenesis by wild type (red line) under the same conditions. D76N fibril formation was accelerated in the presence of carbon nanotubes (green lines), whereas wild type (dashed black line) did not aggregate. C, fibrillogenesis of D76N (red triangles) and wild type (black triangles) carried out under stirring conditions at 37°C in the presence of a Teflon-water interface with 6M human elastin. a.u., arbitrary units.

CARBON NANOTUBES MASSIVELY ENHANCE THE FIBRILLOGENESIS OF D76N (as can be observe in panel B of Figure 1)

It has been previously shown ([Linse et al., 2007](#)), even though at pH 2.5, that nanoparticles enhance the rate of the protein fibrillation by decreasing the lag time of the nucleation. In the particular case of b2m, they found that NPs enhance the probability of appearance of a critical nucleus for nucleation of protein fibrils, with a strong relation between the shorter lag time (nucleation) and the nature of the particle surface.

Graphitic nanomaterials

From the review ([Leo et al., 2015](#))

aminoacids and graphene

- AA-water interactions compete with AA-graphene interactions: water molecules have a negative influence on the binding of AA onto graphitic surface and there is a weakening for the final adsorption energy to graphene
 - Arg (R) (positively charged) > Trp (W) (hydrophobic side chain) > Tyr (Y) (hydrophobic side chain) > His (H) (positively charged) > Gln (Q) (polar) are the residues more able to interact with the surface as they have bigger side chains that can maximize the vdW contact and with the aromatic parts are able to stack on the flat surface
 - Arg (R), Gln (Q), Asn (N) and Lys (K) are the most interacting residues that spontaneously adsorb on graphitic surface
-
- most important interactions come from hydrophilic charged and polar amino acid

Graphene HOMO LUMO orbitals

The interaction geometries of some AA (His, Phe, Tyr, Trp) on the flat surface of graphene are similar in the interplanar distances around 3.3 - 3.5 Å, that recall the pi-pi interactions. In fact, the planar geometry of graphene enhances the pi-pi stacking occurring between the aromatic rings and the surface generating smaller interplanar distances when the aromatic AA adsorb. Consequently, these residues are more stable on planar graphene

protein and graphene

All the biomolecules, studying different domains, tend to approach to the surface regardless of the type of the secondary structure or the starting orientations. And most of them reveals

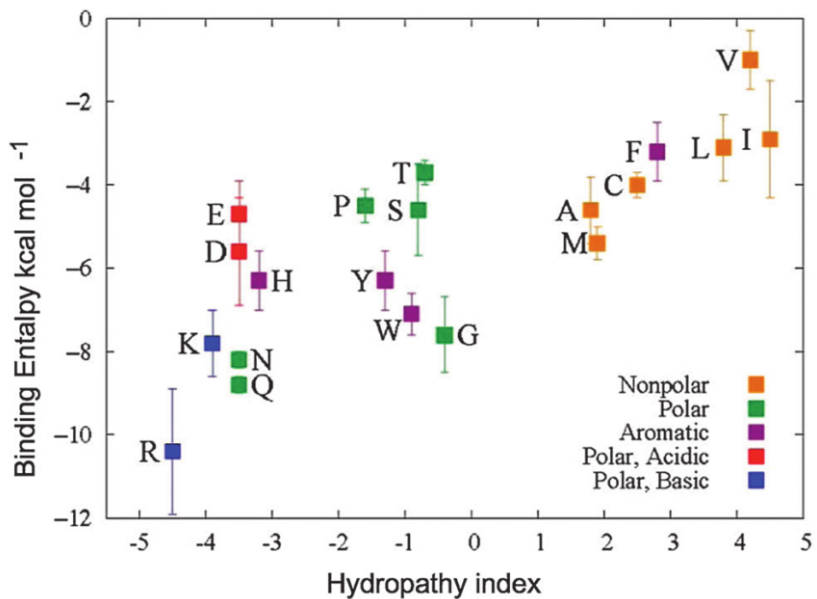


Figure 2: Binding energy of the interacting aa (labeled with the one letter abbreviation) plotted as a function of the hydropathy index.

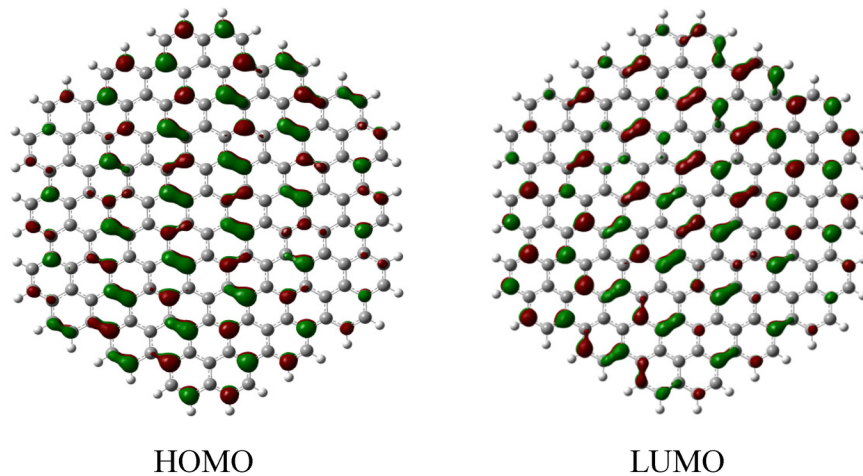


Figure 3: Calculated HOMO and LUMO of H-terminated 6-A-HGNS.

a partial loss of the secondary structure of the protein section that is in contact with the surface. As reported in Figure 4, the worst interaction mode is the one with the long axes of the protein perpendicular to the surface.

INTERESTING: the number of contact in residues linearly correlates with the interaction energy and the protein strain energy calculated for the minimized geometries in different possible orientations.

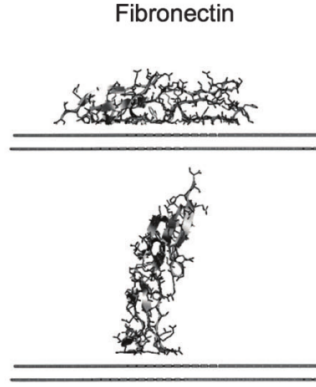


Figure 4: Top is the best orientation, bottom is the worst one.

$$E_{int} = (E_{freeprot} + E_{CNT}) - E_{tot}$$

$$E_{strain} = E_{adsorb} - E_{free}$$

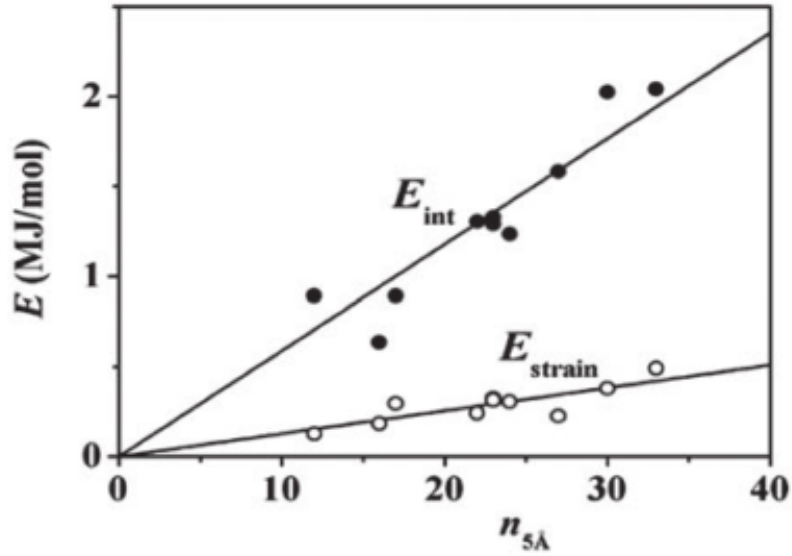


Figure 5: For albumin (white dots) and fibronectin (black dots), the number of contact correlate with different kind of interaction energy. B2m is similar to fibronectin as they both are domain of antiparallel beta sheets

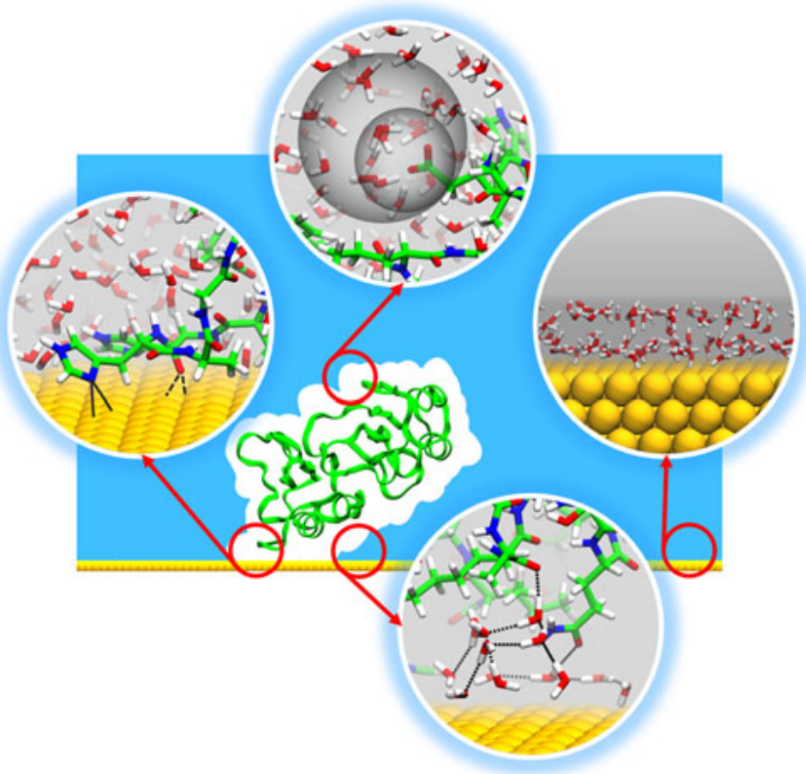


Figure 6: Schematic illustration of protein-surface interactions in aqueous solvent. The main interaction interfaces can be categorized as: protein-surface, protein-solvent, solvent-surface and protein-solvent-surface. The protein-surface interface (depicted in the left circle) includes direct interactions. The interactions can be non-specific such as van der Waals and electrostatic interactions (represented with dashed lines in the figure), or specific such as strong histidine-gold interactions (shown with a continuous line) and even stronger chemisorption interactions. At the protein-solvent interface (depicted in the top circle), the structural and physical properties of the protein and the solvent deviate from those inside the protein and in the bulk solvent, respectively. In particular, water forms layers around the polar and charged residues as depicted by the two spheres in the figure. At the interface, the relative dielectric permittivity of water and of the protein is lower than that of their bulk counterparts. At the solvent-surface interface (depicted in the right circle), the solvent may form structured layers or be completely disordered. On a gold surface, for instance, water forms two ordered layers that are separated by high energy barriers and have a lowered relative dielectric permittivity in the direction normal to the surface. At the protein-solvent-surface interface (depicted in the bottom circle), the interactions involve a complex interplay between the constituents. The protein may make strong indirect interactions with the surface through a stable network of hydrogen bonds (represented by dashed lines) in the adsorption region.

References

- Federica De Leo, Alessandra Magistrato, and Davide Bonifazi. Interfacing proteins with graphitic nanomaterials: from spontaneous attraction to tailored assemblies. *Chemical Society Reviews*, 44(19):6916–6953, 2015. doi: 10.1039/c5cs00190k. URL <https://doi.org/10.1039%2Fc5cs00190k>.
- S. Linse, C. Cabaleiro-Lago, W.-F. Xue, I. Lynch, S. Lindman, E. Thulin, S. E. Radford, and K. A. Dawson. Nucleation of protein fibrillation by nanoparticles. *Proceedings of the National Academy of Sciences*, 104(21):8691–8696, may 2007. doi: 10.1073/pnas.0701250104. URL <https://doi.org/10.1073%2Fpnas.0701250104>.
- P. Patrizia Mangione, Gennaro Esposito, Annalisa Relini, Sara Raimondi, Riccardo Porcari, Sofia Giorgetti, Alessandra Corazza, Federico Fogolari, Amanda Penco, Yuji Goto, Young-Ho Lee, Hisashi Yagi, Ciro Cecconi, Mohsin M. Naqvi, Julian D. Gillmore, Philip N. Hawkins, Fabrizio Chiti, Ranieri Rolandi, Graham W. Taylor, Mark B. Pepys, Monica Stoppini, and Vittorio Bellotti. Structure Folding Dynamics, and Amyloidogenesis of D76N 2-Microglobulin. *Journal of Biological Chemistry*, 288(43):30917–30930, sep 2013. doi: 10.1074/jbc.m113.498857. URL <https://doi.org/10.1074%2Fjbc.m113.498857>.